# Post-buckling Behaviour of Bi-axially Loaded Plates

William J. Supple

Philip J. Wicks

# Post-Buckling Behaviour of Bi-axially Loaded Plates

William J. Supple* and Philip J. Wicks **

## Summary

The post-buckling behaviour of thin plates in bi-axial in-plane compression is investigated. It is found that the addition of the transverse load to the uniaxial loading case has a profound effect not only on the critical loads but also on the post-buckling modes and mode interaction.

## 1. Introduction

The classic work of KOITER (3) has shown the need for an understanding of the behaviour of a structure in its post-classical buckling range since it may exhibit an actual buckling load quite different from that predicted from a theoretical linear eigenvalue analysis. It is well known however, that thin plates loaded in in-plane compression have load-bearing capabilities at loads in excess of the classical buckling stress. SUPPLE (9) however has demonstrated that the feasibility of allowing a plate to function in this post-buckling range is governed by the presence of secondary bifurcation points at which the stable, symmetric equilibrium path may bifurcate into a coupled path. Further, in the presence of certain combinations of initial geometric imperfections the plate may modify its waveform violently by means of a limit point on the equilibrium path. These findings were demonstrated experimentally (6). Working in the context of generalised coordinates after THOMPSON (10), SUPPLE (7) has also shown the types of coupled equilibrium path possible for ideal two degree of freedom structural systems and later (8) how the configurations of these paths coupled with the presence of initial imperfections in the form of the generalised coordinates affect the behaviour in the post-buckling range. From these two complementary studies in generalised coordinates and discrete mechanics the uniaxially loaded plate was shown to fall into the hyperbolic coupled category, the coupled path seen to be rising from a bifurcation point on the secondary uncoupled path.

The present work demonstrates the coupled equilibrium configurations for the plate when an extra orthogonal in-plane stress is applied and any modification this stress may have thereon. The results - although of a fundamental study in their own right - have a direct bearing on thin walled structures, particularly thin-plate assemblages.

* Reader in Structural Engineering, Department of Civil Engineering University of Surrey, U.K.

** Lecturer in Structural Engineering, Space Structures Research Centre, University of Surrey, U.K.

## 2. Equations and Boundary Conditions

We consider the problem of a thin rectangular plate loaded in-plane as shown in figure 1. The support is simple at the boundaries and is such that there are no out-of-plane displacements, the edges translating as straight lines.

These conditions may be expressed as follows:-

i) $(W)_{x=0,a} = 0$

ii) $(W)_{y=0,b} = 0$

iii) $(W,_{xx} + \nu W,_{yy})_{x=0,a} = 0$

iv) $(W,_{yy} + \nu W,_{xx})_{y=0,b} = 0$

v) $(U)_{x=0,a} = \text{constant}$

vi) $(V)_{y=0,b} = \text{constant.}$

where (iii) and (iv) express the condition that the tangential moment vectors at the plate boundaries must be zero for simple support, and where a comma followed by subscripts represents partial differentiation with respect to each subscripted variable in turn.

The Von Karman large deflection equations in the absence of initial geometric imperfections may be written in terms of w(the displacement in the z-direction) and a stress function $\phi$ as follows (11):

$$\nabla^4\phi = E(W,_{xy}^2 - W,_{xx}.W,_{yy}) \qquad .......(2.1)$$

$$\nabla^4 W = \frac{t}{D}(\phi,_{yy} W,_{xx} - 2\phi,_{xy} W,_{xy} + \phi,_{xx} W,_{yy}) \qquad ......(2.2)$$

W being the total out-of-plane displacement from the perfectly flat configuration, $\phi$ being defined by:-

$$\phi,_{yy} = \frac{N_x}{t} = \sigma_x, \quad \phi,_{xx} = \frac{N_y}{t} = \sigma_y, \quad \phi,_{xy} = -\frac{N_{xy}}{t} = \tau_{xy}$$

$$......(2.3)$$

$\sigma_x$ and $\sigma_y$ being normal and $\tau_{xy}$ tangential shear, in-plane, mid-surface stresses and $\nabla^4$ is the biharmonic operator:

$$\frac{\partial^4}{\partial x^4} + \frac{2\partial^4}{\partial x^2 \partial y^2} + \frac{\partial^4}{\partial y^4}$$

D is the flexural stiffness:

$$\frac{Et^3}{12(1-\nu^2)}$$

## 3. Solution of Equations

### 3.1 Solution for stress-function $\phi$ :

We assume a form for the buckling deflection w as the sum of two eigenvectors of the linearized buckling problem, having amplitudes At and Bt:-

$$w = \sin\frac{\pi y}{b}\left(At\sin\frac{n\pi x}{a} + Bt\sin\frac{m\pi x}{a}\right) \qquad \ldots\ldots (3.1)$$

this satisfies the boundary conditions

i) to iv) of section 2.

Writing this for brevity as:

$$w = S_y\,(At\,S_{nx} + Bt\,S_{my}) \qquad \ldots\ldots (3.2)$$

to simplify presentation of ensuing work, where

$$S_{iy} = \mathrm{Sin}\,\frac{i\pi y}{b} \;;\quad C_{ry} = \mathrm{Cos}\,\frac{r\pi y}{b}$$

$$S_{jx} = \mathrm{Sin}\,\frac{j\pi x}{a} \;;\quad C_{sx} = \mathrm{Cos}\,\frac{s\pi x}{a}$$

etc.

and making the necessary substitutions the partial differential equation (2.1) appears as:-

$$\nabla^4\phi = Et^2\left[\frac{\pi^2}{b^2}\cdot C_y^2\left(\frac{An\pi}{a}\cdot C_{nx} + \frac{Bm\pi}{a}\cdot C_{mx}\right)^2 - \frac{\pi^2}{b^2}\,S_y^2\left\{\left(\frac{An^2\pi^2}{a^2}\cdot S_{nx} + \frac{Bm^2\pi^2}{a^2}\cdot S_{mx}\right)\cdot (A.\,S_{nx} + B\,S_{mx})\right\}\right] \qquad \ldots\ldots (3.3)$$

This may be solved exactly for the stress function to give:

$$\phi = \frac{EA^2t^2}{32}\left\{\frac{n^2b^2}{a^2}C_{2y} + \frac{a^2}{n^2b^2}C_{2nx}\right\} + \frac{Ea^2ABt^2}{4b^2}\left\{\frac{C_{(n+m)x}}{(n+m)^2} - \frac{C_{(n-m)x}}{(n-m)^2}\right\} \qquad \ldots\ldots \text{continued..}$$

$$-\frac{Ea^2b^2ABt^2}{4}.C_{2y}\left\{\alpha C_{(n+m)x} + \beta C_{(n.m)x}\right\}$$

$$+\frac{EB^2t^2}{32}\left\{\frac{m^2b^2}{a^2}C_{2y} + \frac{a^2}{m^2b^2}C_{2mx}\right\} - \frac{\lambda_x}{8bt}(2y-b)^2$$

$$-\frac{\lambda_y}{8at}(2x-a)^2 \qquad .. \qquad .. \qquad .. \qquad ....(3.4)$$

where

$$\alpha = \frac{(n-m)^2}{\{(n+m)^2b^2+4a^2\}^2} \quad ; \qquad \beta = \frac{(n+m)^2}{\{(n-m)^2b^2+4a^2\}^2}$$

and $\lambda_x$, $\lambda_y$ represent total applied loads in the x and y directions respectively, i.e.

$$\lambda_y = \int_o^a N_y \, dx \quad ; \quad \lambda_x = \int_o^b N_x \, dy$$

Deriving the midsurface stress resultants from the stress function and using the strain-displacement relations and generalised Hooke's law, expressions may be obtained for u and v, the displacements in the x and y directions. With this done it is found that boundary conditions v) and vi) are satisfied with no restriction on n or m.

## 3.2 Ritz-Galerkin Procedure:

We may substitute $\phi$ and w, after appropriate differentiations, into the equilibrium equation (2.2). In general this equation is not exactly satisfied due to the approximate nature of the chosen w but will have a residual R, say. Equating to zero the excess virtual energy defined as:

$$\int_o^a \int_o^b R.w.dy\, dx$$

we obtain two approximate equations of post-buckling equilibrium.

Carrying out these operations the latter equations appear as:

$$\left[3(1-\nu^2)\,\frac{a^2b^2}{16n^2}\left\{\left(\frac{n^4}{a^4}+\frac{1}{b^4}\right)A^2+\left(\frac{n^2m^2}{a^4}+4K\right)B^2\right\}\right.$$

$$\left.+\,\frac{a^2b^2}{4n^2}\left(\frac{n^2}{a^2}+\frac{1}{b^2}\right)^2-\left(\lambda_x b+\frac{\lambda_y a}{n^2}\right)\frac{1}{4\pi^2 D}\right]A \;=\; 0 \qquad \ldots\ldots\ (3.5i)$$

$$\left[3(1-\nu^2)\,\frac{a^2b^2}{16m^2}\left\{\left(\frac{m^4}{a^4}+\frac{1}{b^4}\right)B^2+\left(\frac{n^2m^2}{a^4}+4K\right)A^2\right\}\right.$$

$$\left.+\,\frac{a^2b^2}{4m^2}\left(\frac{m^2}{a^2}+\frac{1}{b^2}\right)^2-\left(\lambda_x b+\frac{\lambda_y a}{m^2}\right)\frac{1}{4\pi^2 D}\right]B \;=\; 0 \qquad \ldots\ldots\ (3.5ii)$$

where

$$K=\frac{1}{b^4}+\frac{\alpha}{4}(n-m)^2+\frac{\beta}{4}(n+m)^2$$

We now specify that the average applied normal stresses on the y-facing boundaries are some factor $\mu$ times the average applied normal stresses on the x-facing boundaries i.e.

$$\left(\frac{\lambda_x}{bt}\right)=\mu\left(\frac{\lambda_y}{at}\right)$$

and for convenience we introduce the notation

$$\lambda_x=\Lambda$$

$$\lambda_y=\left(\frac{\mu a}{b}\right)\Lambda$$

The loading terms in equations (3.5i) and (3.5ii) then appear as:

$$\Lambda\left(b+\frac{\mu a^2}{bn^2}\right)$$

and

$$\Lambda\left(b+\frac{\mu a^2}{bm^2}\right)$$

respectively.

### 3.3 Post-Buckling Solutions

There are three solutions of the equilibrium equations (3.5) characterized by

i) $A = 0,\ B \neq 0$
ii) $A \neq 0,\ B = 0$
iii) $A \neq 0,\ B \neq 0$

the first two define the uncoupled buckling modes, the latter the coupled mode.

#### 3.3.1 Uncoupled modes:

Putting $A \neq 0$, $B = 0$ and $A = 0$, $B \neq 0$ into equations (3.5) yield the uncoupled modes:

$$\frac{\Lambda}{4\pi^2 D}\left(b + \frac{\mu a^2}{bn^2}\right) = 3(1-\nu^2)\frac{a^2b^2}{16n^2}\left(\frac{n^4}{a^4} + \frac{1}{b^4}\right)A^2 + \frac{a^2b^2}{4n^2}\left(\frac{n^2}{a^2} + \frac{1}{b^2}\right)^2 \qquad \text{..... (3.6i)}$$

$$\frac{\Lambda}{4\pi^2 D}\left(b + \frac{\mu a^2}{bm^2}\right) = 3(1-\nu^2)\frac{a^2b^2}{16m^2}\left(\frac{m^4}{a^4} + \frac{1}{b^4}\right)B^2 + \frac{a^2b^2}{4m^2}\left(\frac{m^2}{a^2} + \frac{1}{b^2}\right)^2 \qquad \text{..... (3.6ii)}$$

noting that with $\mu = 0$ the above reduce to the corresponding equations for the uniaxial case (7).

Putting $A = 0$ in (3.6i) and $B = 0$ in (3.6ii) the loads at which two uncoupled equilibrium paths bifurcate from the load axis are obtained. We designate these modes as the primary and secondary uncoupled modes, the former occuring at the lower branching load. Both loads are given by the expression :

$$\Lambda = \frac{\pi^2 D}{\left(\frac{b+\mu a^2}{bn^2}\right)} \frac{a^2b^2}{n^2}\left(\frac{n^2}{a^2} + \frac{1}{b^2}\right)^2 \qquad \text{...... (3.7)}$$

where we may select two distinct values of n representing our m, n values in the analysis.

Dividing both sides by bt gives:

$$\sigma_{cr} = \frac{\pi^2 E}{12(1-\nu^2)} \left(\frac{t}{b}\right)^2 \frac{(n^2/\gamma^2 + \gamma)^2}{(n^2 + \mu\gamma^2)} \qquad \ldots\ldots (3.8)$$

where $\gamma$ is the aspect ratio of the plate a/b.

The latter part of equation (3.8) corresponds to a buckling stress coefficient $K'_c$ defined by:

$$K'_c = \frac{(n^2/\gamma^2 + 1)^2}{n^2/\gamma^2 + \mu} \qquad \ldots\ldots\ldots (3.9)$$

which is in agreement with the linear solution by BULSON (2) after BRYAN (1), for here we have assumed the plate buckles in one half sine-wave in the y-direction.

BULSON also shows that $K'_c$ minimizes at a value of aspect ratio given by:

$$\gamma = n/\sqrt{1-2\mu} \qquad (\mu < 0.5)$$

giving $K'_c$ a minimum value of :

$$(K'_c)\min = 4(1-\mu) \qquad (\mu < 0.5)$$

and that,

$$\lim_{\gamma \to \infty} K'_c = \frac{1}{\mu} \qquad (\mu \geq 0.5)$$

Further by inspection of equation (3.9) $K'_c$ is seen to be discontinuous at $\gamma = n/\sqrt{-\mu}$.

It can be shown by equating expressions for $K'_c$ that coincident buckling in n and m half-sine-waves occurs at a value of $\gamma$ given by:

$$\gamma^2 = \frac{\mu(n^2+m^2) + \sqrt{\mu^2(n^2+m^2)^2 + 4(1-2\mu)m^2n^2}}{2(1-2\mu)} \qquad \ldots\ldots (3.10)$$

which with $\mu=0$ reduces to the well-known expression for coincident buckling in the uniaxial case, $\gamma = \sqrt{mn}$

Figure 2 shows plots of $K'_c$ against plate aspect ratio $\gamma$ for various values of wave number n and orthogonal stress ratio $\mu$.

3.3.2 Coupled Modes:

Elimination of the load term between equations (3.5i) and (3.5ii) gives the projection of the coupled mode onto the A-B plane as:

$$\left[\frac{n^4+\gamma^4}{n^2+\mu\gamma^2} - \frac{n^2m^2+K'}{m^2+\mu\gamma^2}\right]A^2 + \left[\frac{n^2m^2+K'}{n^2+\mu\gamma^2} - \frac{m^4+\gamma^4}{m^2+\mu\gamma^2}\right]B^2$$

$$= \frac{4}{3(1-\nu^2)}\left[\frac{(m^2+\gamma^2)^2}{m^2+\mu\gamma^2} - \frac{(n^2+\gamma^2)^2}{n^2+\mu\gamma^2}\right] \qquad \text{........ (3.11)}$$

where

$$K' = 4a^4K$$

Thus it is of the form:

$$K_1A^2 + K_2B^2 = K_3 \qquad \text{....... (3.12)}$$

and is the equation of a general conic representing a number of forms depending on the signs $K_1$, $K_2$ and $K_3$.

For fixed values of n and m these coefficients may be represented in $\mu - \gamma - K_i$ space as surfaces. We are interested in the curves of intersection with the $\mu - \gamma$ plane since it is across these that the signs of the coefficients will change.

By inspection of the coefficient of equation (3.11) we further note that all the $K_i$ surfaces have discontinuities on the $\mu - \gamma$ plane defined by the curves.

$$\mu = \frac{-n^2}{\gamma^2}, \qquad \mu = \frac{-m^2}{\gamma^2} \qquad \text{...... .. (3.13)}$$

Equating each of the $K_i$ coefficients to zero in turn and solving for $\mu$ the curves of intersection appear as:

$$\mu\Big|_{K_1=0} = \frac{n^2K' - m^2\gamma^4}{\gamma^2(n^4+\gamma^4-n^2m^2-K')} \qquad \text{...... (3.14i)}$$

$$\mu\Big|_{K_2=0} = \frac{n^2\gamma^4 - m^2K'}{\gamma^2(n^2m^2+K'-m^4-\gamma^4)} \qquad \text{...... (3.14ii)}$$

$$\mu\Big|_{K_3=0} = \frac{\gamma^4 - m^2n^2}{\gamma^2(n^2+2\gamma^2+m^2)} \qquad \text{...... (3.14iii)}$$

the latter equation being a re-statement of the condition for coincident buckling given previously by equation (3.10)

By superposition of all these curves we may establish sets of $\mu$, $\gamma$ for given n,m within which a particular combination of signs and hence a particular form of coupled mode for equation (3.12) will occur. A plot of these curves on the $\mu$-$\gamma$ plane is shown in figure 3.

We observe that for certain combinations of $\mu$ and $\gamma$ the coupled mode forms a closed transition path (in the form of an ellipse when projected on to the A-B plane in the $\Lambda$-A-B space) between the uncoupled buckling modes. This would indicate a change in mode form for the perfect plate in the post-buckling range. For other combinations of $\mu$ and $\gamma$ either no coupled solution exists or a coupled mode which bifurcates from the secondary uncoupled mode. The latter has been shown to have importance when imperfections are present (6), (8).

Writing for brevity:

$$K_4 = \frac{n^4+\gamma^4}{n^2+\mu\gamma^2}, \qquad K_5 = \frac{n^2m^2+K'}{n^2+\mu\gamma^2}$$

$$K_6 = \frac{1}{4\gamma^2}\frac{(n^2+\gamma^2)^2}{n^2+\mu\gamma^2}, \qquad K_7 = \frac{m^4+\gamma^4}{m^2+\mu\gamma^2}$$

$$K_8 = \frac{n^2m^2+K'}{m^2+\mu\gamma^2}, \qquad K_9 = \frac{1}{4\gamma^2}\frac{(m^2+\gamma^2)^2}{m^2+\mu\gamma^2}$$

and

$$\bar{\Lambda} = \frac{\Lambda b}{4\pi^2 D}$$

whereupon the coupled equation becomes:

$$(K_4-K_8)A^2 + (K_5-K_7)B^2 = \frac{16\gamma^2}{3(1-\nu^2)}(K_9-K_6) \qquad \ldots\ldots\ (3.15)$$

and the uncoupled modes are:

$$\bar{\Lambda} = \frac{3(1-\nu^2)}{16\gamma^2}.K_4A^2 + K_6 \qquad \ldots\ldots\ (3.16i)$$

$$\bar{\Lambda} = \frac{3(1-\nu^2)}{16\gamma^2}.K_7B^2 + K_9 \qquad \ldots\ldots\ (3.16ii)$$

Elimination of B or A between the two equations (3.5) yields the projections of the coupled mode onto the $\bar{\Lambda}$-A or $\bar{\Lambda}$-B planes respectively, these being:

$$\bar{\Lambda} = \frac{3(1-\nu^2)}{16\gamma^2} \frac{(K_4K_7-K_5K_8)}{K_7-K_5} A^2 + \frac{K_6K_7-K_5K_9}{K_7-K_5} \quad \ldots\ldots\ (3.17i)$$

$$\bar{\Lambda} = \frac{3(1-\nu^2)}{16\gamma^2} \frac{(K_5K_8-K_4K_7)}{K_8-K_4} B^2 + \frac{K_6K_8-K_4K_9}{K_8-K_4} \quad \ldots\ldots\ (3.17ii)$$

These are seen to be parabolic as established for the uniaxial case by SUPPLE (9). The secondary bifurcation loads may be established from these latter equations, and are simply the constant terms.

## 4. Conclusions

Critical loads and post-buckling paths have been determined for thin flat rectangular plates under bi-axial loading. Interest has been centred on the coupled buckling interaction between pairs of buckling modes. The application of the transverse axial load to the uni-axial loading case is seen to modify the value of the plate aspect ratio at which simultaneous buckling occurs. Furthermore, the form of the coupled post-buckling equilibrium paths are also altered. Under certain conditions it is shown that the coupled mode forms a closed transition path betweem the uncoupled buckling mode paths and would thus produce a mode-switching effect in the post-buckling range.

## Appendix: References

1. Bryan, G.H., Proc. London Math. Soc. (1891) V22 pp54.

2. Bulson, P.S. 'The Stability of Flat Plates,' Chatto and Windus, 1970. pp 57.

3. Koiter, W.T. Dissertation, Delft, Holland (1945), English translation NASA, TT, F10, 833 (1967).

4. Nakamura, T. and Uetani, K., Int. J. Mech. Sci. (1979) V21, pp265.

5. Sharman, P.W., and Humpherson, J. Aero Journ. Royal Aero Soc. (1968) V72, pp 431.

6. Supple, W.J. Ph.D. thesis, University of London (1966)

7. Supple, W.J. Int. J. Mech. Sci. (1967) V9 pp 97.

8. Supple, W.J. Int. J. Mech. Sci. (1968) V10 pp 737.

9. Supple, W.J. Int. J. Solids Structures (1970) V6 pp 1243.

10. Thompson, J.M.T. J. Mech. Phys. Solids (1963), V11 pp 13.

11. Timoshenko, S.P. and Woinowsky-Kreiger, S. Theory of Plates and Shells Int. Student Edition. McGraw Hill, 1959. pp. 415.

## Appendix: Notation

| | |
|---|---|
| $x$, $y$, $z$ - | coordinate directions. |
| $u$, $v$, $w$ - | displacements. |
| $a$, $b$, $t$ - | plate dimensions |
| $E$, $\gamma$ - | elastic properties of plate material. |
| $\gamma$ - | aspect ratio of plate. |
| $D$ - | plate rigidity. |
| $N_x$, $N_y$, $\lambda_x$, $\lambda_y$, $\sigma_x$, $\sigma_y$ - | 'loading' parameters in specified directions. |
| $\bar{\Lambda}$, $\Lambda$ - | overall loading parameters. |
| $\mu$ - | parameter relating longitudinal and transverse loading. |
| $n$, $m$ - | numbers of half-sine-waves in wave modes. |
| $\phi$ - | stress function. |
| $A$, $B$ - | wavemode amplitudes as ratios of plate thickness. |
| $K'_c$ - | buckling stress coefficient. |
| $K_i$ - | coefficients in equations. |

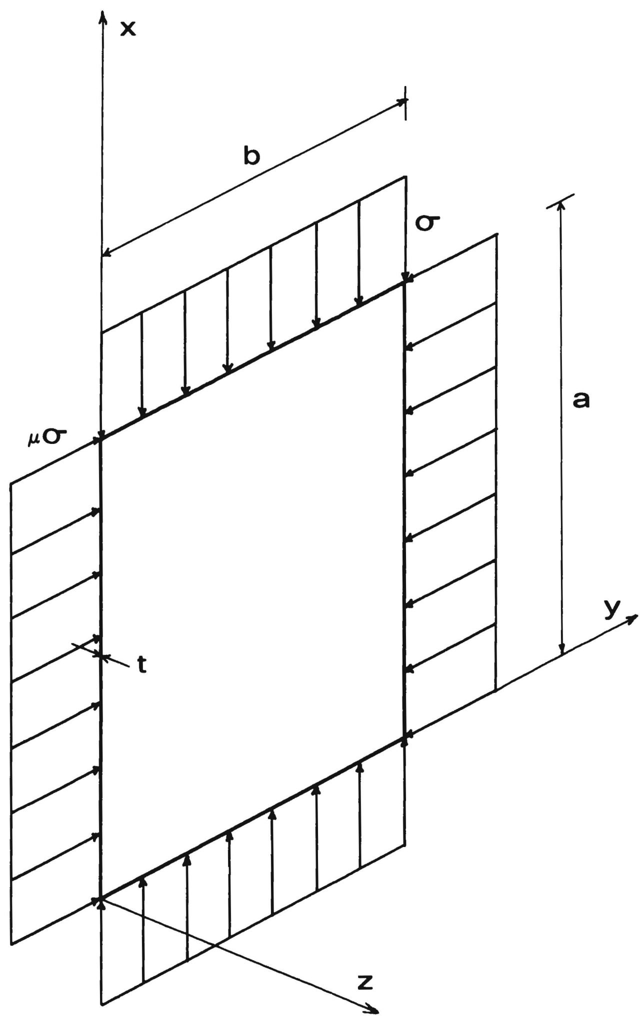


Figure 1. Plate dimensions and loading.

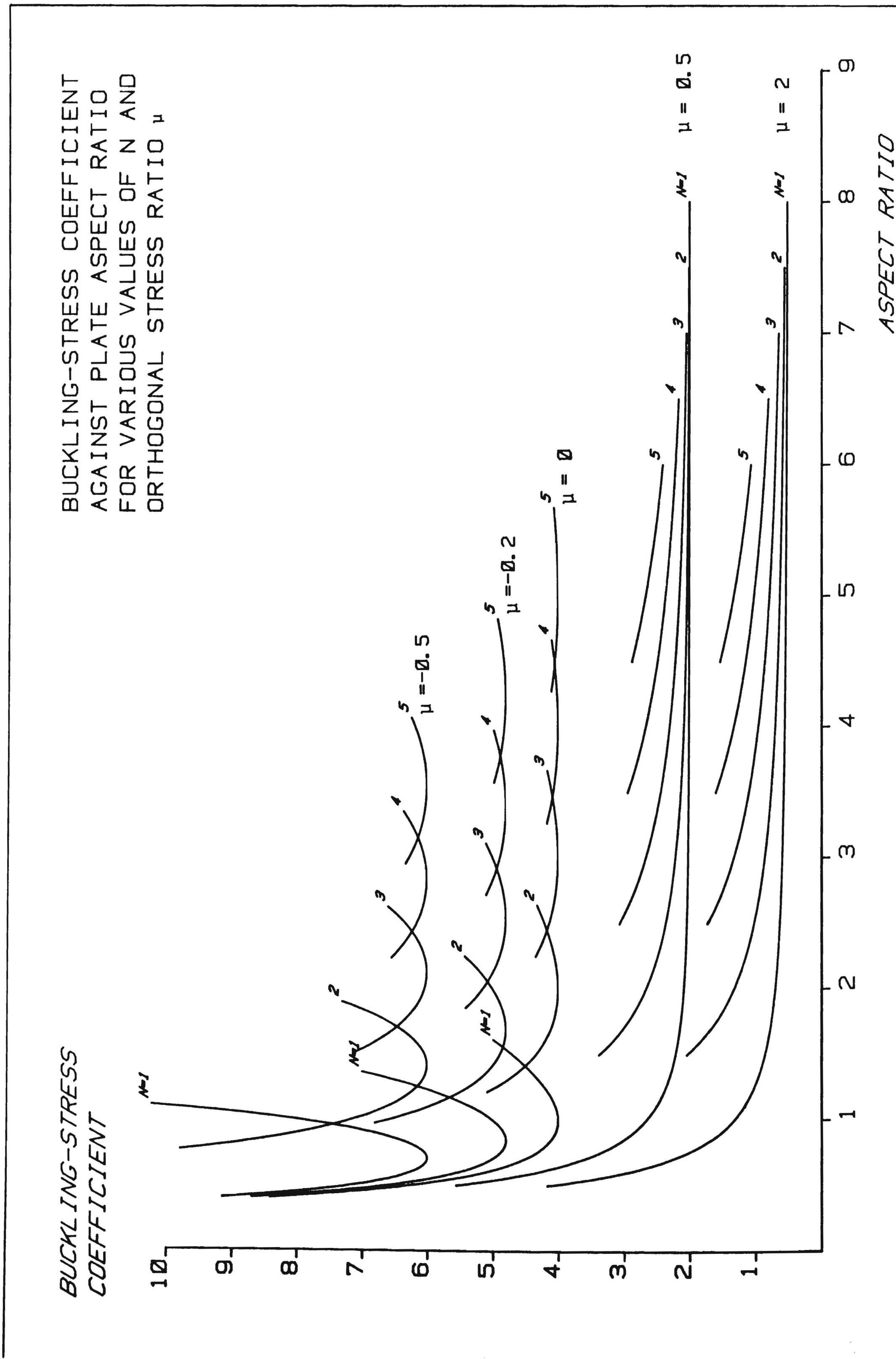
BUCKLING-STRESS COEFFICIENT AGAINST PLATE ASPECT RATIO FOR VARIOUS VALUES OF N AND ORTHOGONAL STRESS RATIO μ
BUCKLING-STRESS COEFFICIENT
ASPECT RATIO
μ = -0.5
μ = -0.2
μ = 0
μ = 0.5
μ = 2
N=1
2
3
4
5
10
9
8
7
6
5
4
3
2
1
1
2
3
4
5
6
7
8
9

Figure 2

PLOTS OF K1, K2 AND K3=Ø CURVES N=1, M=2

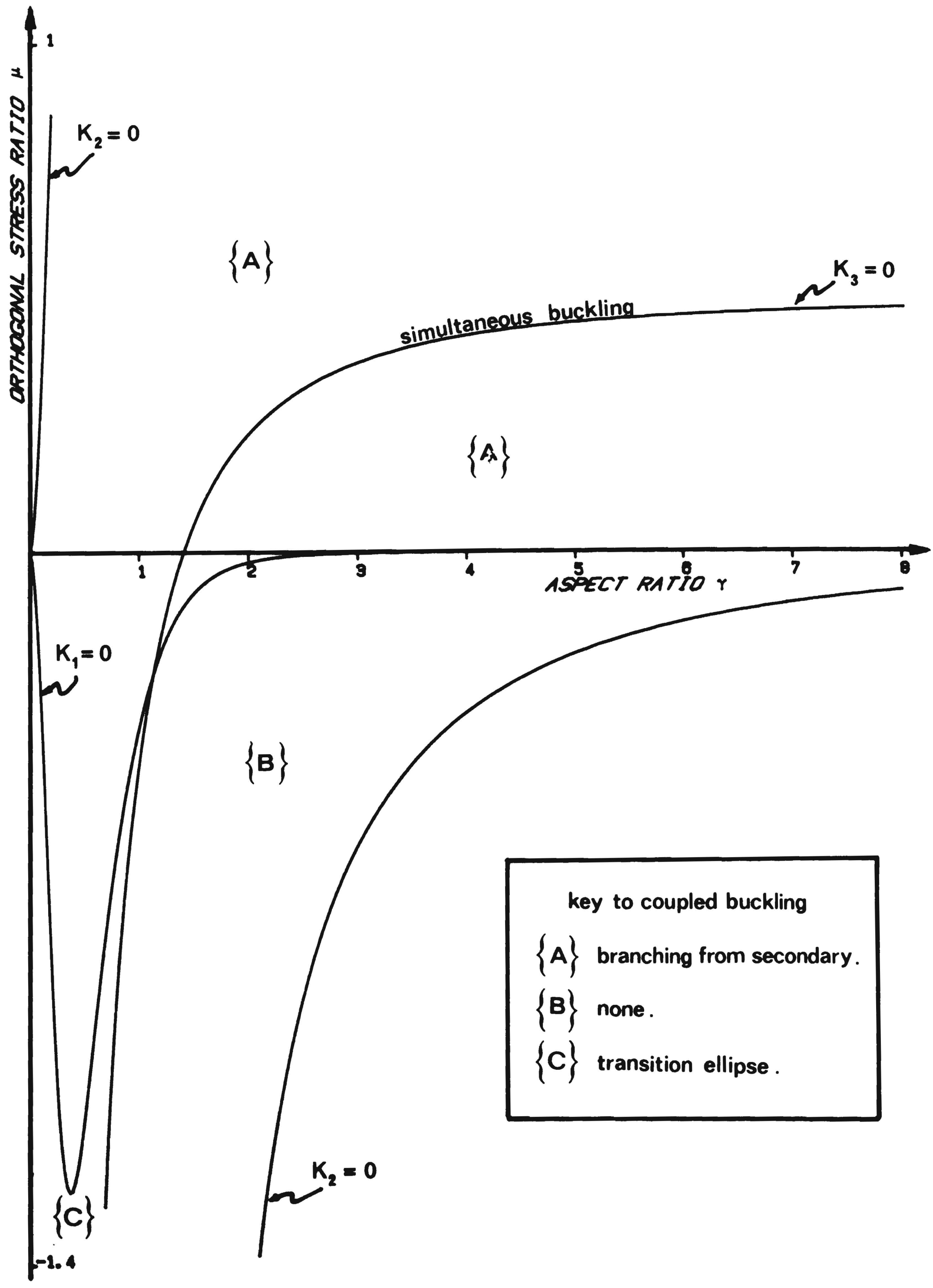


Figure 3.